

irradiated with He/Ne laser for different periods of time. Spikes formed by He/Ne laser irradiation were washed with acetone and measured. These results are summarized in Table III.

**Acknowledgment.** We are deeply indebted to Dr. E. Dolan for the laser setup for two-photon photopolymerization and to Dr. S. Kumar and Dr. J. Paczkowski

for valuable discussions. This work has been supported by the National Science Foundation, Division of Materials Research (DMR 8702733). We are grateful for this support.

**Registry No.** 4, 100239-68-7; 5, 98883-30-8; 6, 135823-65-3; 9, 135823-64-2; TMPTA, 15625-89-5; *N*-phenylglycine, 103-01-5.

## Third-Order Optical Nonlinearities of Model Compounds Containing Benzobisthiazole, Benzobisoxazole, and Benzbisimidazole Units

Bruce A. Reinhardt,\* Marilyn R. Unroe, and Robert C. Evers

*Polymer Branch, Nonmetallic Materials Division, Wright Laboratory, Wright-Patterson AFB, Ohio 45433-6533*

Mingtang Zhao, Marek Samoc, and Paras N. Prasad\*

*Photonics Research Laboratory, Department of Chemistry, State University of New York at Buffalo, Buffalo, New York 14214*

Mark Sinsky

*SYSTRAN Corporation, Dayton, Ohio 45324*

*Received March 12, 1991. Revised Manuscript Received July 22, 1991*

As part of a continuing study, a series of highly conjugated aromatic benzobisthiazole, benzobisoxazole, and *N,N*-diphenylbenzbisimidazole model compounds were synthesized, and their third-order nonlinear optical properties investigated by using subpicosecond degenerate four-wave mixing. Measurements were made at 602 nm on THF solutions, vacuum-deposited films, or melt-quenched films. In all but one material, the third-order effect was determined to be instantaneous within the employed temporal resolution, suggesting dominance of electronic nonlinearity. From the experimental data it was possible to formulate structure-nonlinear optical property correlations and demonstrate that the molecular second hyperpolarizability can be increased almost 3 orders of magnitude by simple structural modifications.

### 1. Introduction

A previously coordinated effort of our two laboratories<sup>1</sup> involved the synthesis and third-order nonlinear optical (NLO) susceptibility measurements on a number of aromatic heterocyclic model compounds. This study provided structure-NLO property information for a series of benzothiazole, benzoxazole, and *N*-phenylbenzimidazole molecules with a variety of other structural components. Systematic structure-NLO property correlations were formulated for these materials that demonstrated the effects of the following on the third-order nonlinear susceptibility: (1) nature of the heterocycle, (2) effective conjugation length, (3) electron richness of the nonheterocyclic structural units, and (4) two-dimensional  $\pi$ -conjugation effects.

In general, heterocyclic conjugated molecules can enhance third-order NLO activity via a number of routes. The incorporation of five-membered heterocyclic rings into the molecular backbone tends to minimize steric interactions, promoting planarity and thus increasing the effective  $\pi$ -conjugation length. In addition, in terms of a coupled anharmonic oscillator model<sup>2</sup> the participation of the atomic orbitals of the heterocyclic atoms in the  $\pi$ -system

increases the orbital overlap between units, which leads to either a larger coupling constant or a larger local anharmonicity of the molecular oscillator.

As an extension of our initial study it was deemed necessary to study heterocyclic model compounds containing three fused rings. The existence of such a highly conjugated, rigid structural moiety in the repeat unit of rigid-rod polymers such as PBT<sup>3</sup> is postulated to be a major contributor to the polymer's third-order NLO activity. Not only do such highly conjugated structures enhance NLO activity, but they also tend to impart high melting points and greatly reduced solubility to any molecules into which they are incorporated. The purpose of the current research is therefore 4-fold: first, to synthesize attempt to optimize  $\gamma$  for PBT-like fused ring model compounds; second, to improve solubility/processibility characteristics of these materials to acquire samples suitable for measurements; third, to investigate the third-order NLO behavior of these materials by degenerate four-wave mixing (DFWM); finally, to develop structure-NLO property correlations similar to those developed previously.<sup>1</sup> It was postulated that experimental data of this type would provide baseline data for the synthesis of

(1) Zhao, M.; Samoc, M.; Prasad, P.; Reinhardt, B.; Unroe, M.; Prazak, M.; Evers, R. *Chem Mater.* 1990, 2, 670.

(2) Prasad, P. N.; Perrin, E.; Samoc, M. *J. Chem. Phys.* 1989, 91, 2360.

(3) Rao, D. N.; Swiatkiewicz, J.; Chopra, P.; Ghoshal, S. K.; Prasad, P. N. *Appl. Phys. Lett.* 1986, 48, 1187. Lee, C. Y.; Swiatkiewicz, J.; Prasad, P. N.; Mehta, R.; Bai, S. J. *Polymer* 1981, 32, 1195.

new third-order nonlinear polymers with not only increased nonlinearity but also with greatly improved solubility and processibility.

For clarity, we recall the definitions relating to the nonlinear optical properties that are used throughout the paper. The third-order nonlinearity is usually expressed as a cubic term in the expansion of the material polarization  $\mathbf{P}$  versus the electric field  $\mathbf{E}$  acting on the material:

$$\mathbf{P} = \chi^{(1)}\mathbf{E} + \chi^{(2)}\mathbf{E}\mathbf{E} + \chi^{(3)}\mathbf{E}\mathbf{E}\mathbf{E} + \dots \quad (1)$$

The susceptibilities  $\chi^{(n)}$  are tensors of the  $n + 1$  rank and terms  $\mathbf{E}\mathbf{E}$  and  $\mathbf{E}\mathbf{E}\mathbf{E}$  are tensors of second and third rank, respectively. It must be kept in mind that the above definition is oversimplified and does not take into account the dispersion effects that can be properly accounted for only when the products in eq 1 are changed to convolutions. Fourier transformation then leads to  $\chi^{(n)}$  as functions of frequencies of interacting field components. (For example see: Shen, Y. R. *The Principles of Nonlinear Optics*; Wiley: New York, 1984.) Our interest is primarily focused on the third-order susceptibility  $\chi^{(3)}(-\omega; \omega, \omega, \omega)$ , which describes the process of degenerate four-wave mixing and is important for phenomena such as phase conjugation, nonlinear refractive index change, etc. Other third-order nonlinear processes may be related to respective nonlinear susceptibilities. For example, the third harmonic generation (THG) process is described by  $\chi^{(3)}(-3\omega; \omega, \omega, \omega)$ . However, the relationship between different susceptibilities of the same order is not straightforward since different material resonances may contribute to them. One can note here that the DFWM susceptibility is mostly affected by material resonances close to  $2\omega$ ,  $\omega$ , and zero frequency (low-frequency) material modes while the THG susceptibility is primarily affected by resonances close to  $3\omega$ ,  $2\omega$ , and  $\omega$ .

On the microscopic (molecular) level, eq 1 is replaced by the following:

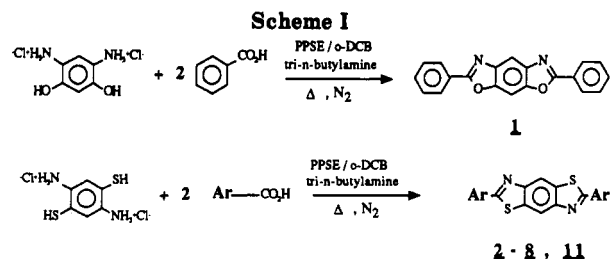
$$\mathbf{p} = \alpha\mathbf{E} + \beta\mathbf{E}\mathbf{E} + \gamma\mathbf{E}\mathbf{E}\mathbf{E} + \dots \quad (2)$$

where  $\mathbf{p}$  is the induced dipole moment and the polarizability  $\alpha$  and the hyperpolarizabilities  $\beta$  and  $\gamma$  behave similarly to the bulk susceptibilities discussed above. The relationship between the polarizabilities of different order and the corresponding macroscopic susceptibilities involve accounting for molecular orientations in the material (in the case of liquids or amorphous solids this is done by orientational averaging) and for local field factors.<sup>13</sup>

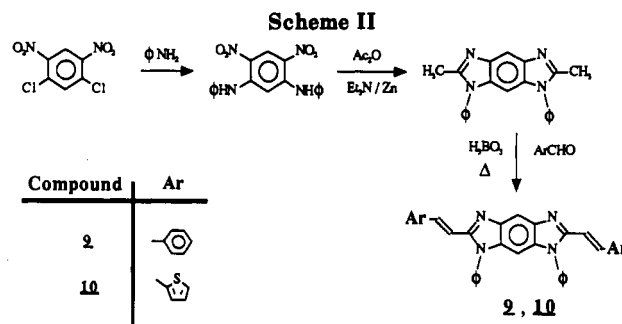
An additional complicating factor that arises in the interpretation of third-order nonlinearities is that of involvement of molecular oscillations and librations (phonons in the solid phase). These processes can dominate the nonlinearity if appropriate frequency Fourier components are present in the combinations of input frequencies as in the CARS experiment or in the case of impulsive scattering. In our case, however, the electronic nonlinearity can be expected to dominate the four-wave mixing process. This assumption appears to be valid because the molecular reorientations should be minimized in solid films and with the pulse length used (400 fs) the pulses are monochromatic enough not to excite internal molecular oscillations by impulsive scattering.

## 2. Results and Discussion

**2.1. Synthesis.** The synthesis of the benzobisoxazole and benzobisthiazole model compounds was carried out using a procedure similar to that described previously for other NLO model compounds.<sup>1</sup> The trimethylsilyl polyphosphate (PPSE) catalyzed condensation (Scheme I) of the appropriate diaminophenol or dithiophenol monomer



Compound	Ar
2	
3	
4	
5	
6	
7	
8	
11	



produced model compounds 2–8 and 11 of high purity and with yields ranging from 49 to 92% (procedure A). In all cases the model compounds exhibited physical properties and gave analyses consistent with the proposed structures. The physical properties and analyses for all model compounds synthesized are summarized in Table I.

The benzobisimidazole model compounds 9 and 10 were synthesized in 40 and 45% yields, respectively, by the boric acid catalyzed condensation of the appropriate 2,6-dimethyl compound with either benzaldehyde or 2-thiophenecarboxaldehyde as depicted in Scheme II (procedure B).

**2.2. NLO Characterization.** The  $\gamma$  and  $\chi^{(3)}$  values obtained from DFWM measurements for all the molecules investigated in this study are listed in Table 2. Also listed are the positions of the dominant absorption peaks observed in the UV-visible (UV-vis) spectra of the model compounds measured from THF solutions. Generally, these absorption transitions are either the  $n\pi^*$  or  $\pi\pi^*$  type, with the  $n\pi^*$  transitions corresponding to the lower energies but smaller oscillator strengths. On the basis of the description of the molecular hyperpolarizabilities in the terms of the sum-over-states approach, it is expected that the contribution from  $\pi\pi^*$  transitions to  $\gamma$  is more than that from low-lying  $n\pi^*$  transitions. The relative importance of these two types of transitions cannot be assessed with any confidence without the knowledge of all terms entering the sum-over-states expression.

All the molecules investigated in this paper are considered to be one-dimensionally conjugated except the *N,N*-

Table I. Properties of Benzobisazole Model Compounds

compd	synth procedure	mp, °C (solvent) yield <sup>a</sup>	lit. mp, °C (solvent) lit. ref	elem anal or CARN		EIMS <sup>b</sup> <i>m/z</i> , %	
				calcd	found		
1	A	332-334 (toluene) 76%	335-336 (sublimation) 4	known compound	28999-67-9		
2	A	300-302 (toluene) 92%	303-304 (toluene) 5	known compound	13399-13-8		
3	A	410-412 (DSC) (DMAc) 50%	260 <sup>c</sup> (pyridine) 6	% C % H % N	62.22 3.19 18.46	62.24 3.20 18.48	346 (100, M <sup>+</sup> )
4	A	323-325 (xylene) 67%		% C % H % N	53.90 2.26 7.86	54.06 2.41 7.81	356 (100, M <sup>+</sup> )
5	A	126-128 (IPA/CH <sub>2</sub> Cl <sub>2</sub> ) 52%		% C % H % N % S	74.33 9.56 2.89 6.61	74.21 9.14 2.79 6.51	969 (3, M <sup>+</sup> ) 43 (100)
6	A	302-304 (DMF) 78%	264 <sup>d</sup> (butanal) 7	% C % H % N	72.69 4.07 7.07	72.51 4.31 7.13	396 (84, M <sup>+</sup> ) 395 (100)
7	A	321-324 (DMF) 65%		% C % H % N	58.79 2.96 6.86	58.51 3.10 6.82	408 (34, M <sup>+</sup> ) 406 (100)
8	A	301-303 (xylene) 51%		% C % H % N	78.80 4.41 5.11	78.81 4.75 5.04	548 (72, M <sup>+</sup> ) 547 (100)
9	B	325-327 (diglyme) 40%	325-327 (acetic acid) 8	known compound	63405-78-7		
10	B	301-302 (toluene) 45%		% C % H % N	72.97 4.21 10.64	73.10 4.41 10.60	526 (53, M <sup>+</sup> ) 77 (100)
11	A	255-256 (xylene) 49%		% C % H % N	62.48 4.89 4.86	62.89 5.01 4.81	576 (15, M <sup>+</sup> ) 545 (100)

<sup>a</sup> Purified yield. <sup>b</sup> Electron impact mass spectral analysis performed by WL/MSLA, Wright-Patterson AFB, OH. <sup>c</sup> The compound of this molecular structure has been assigned the Chemical Abstracts Registry Number (CARN) 109591-64-2. However, due to the relatively low melting point reported in the literature,<sup>6</sup> it is believed that the initially reported compound is not the correct "linear isomer". <sup>d</sup> Again it is believed that the compound reported in the literature<sup>7</sup> CARN 122583-88-4 is not the linear isomer.

diphenylbenzobisimidazoles. In the one-dimensional systems it is expected that the optical bandgap becomes narrower as more aromatic units are introduced into the molecular backbone to lengthen its  $\pi$ -conjugation. On the other hand, the orientationally averaged  $\gamma$  for a one-dimensional molecule is generally believed to be dominated by  $\gamma$  along the molecular backbone. In a simple picture described by Rustagi et al.,<sup>9</sup>  $\chi^{(3)}$  is inversely proportional to the sixth power of the bandgap of the molecule. As a result, a molecule with a smaller bandgap will have a larger  $\chi^{(3)}$  and  $\gamma$  value. The bandgap in turn depends on the degree to which the  $\pi$  electrons are delocalized along the molecular backbone. Obviously, the larger the conjugation length, the smaller the bandgap and the larger the hyperpolarizabilities. A discussion of the conjugation length change for specific molecules and its influence on the molecular nonlinearity follows.

In the following discussion, the molecules studied are divided into groups by their similarity in chemical structure. The molecules in each group differ by only one "functional group". The "functional groups" in the present

paper refer to those small units such as various kinds of heterocyclic aromatics, double bonds, and substituted side groups, all of which are incorporated into various molecular building blocks to build larger molecules.

**2.2.1. Roles of Benzobisthiazole and Benzobisoxazole.** In a previous paper<sup>1</sup> it was concluded that benzothiazole is better than benzoxazole as a nonlinear optical block unit because of the participation of the empty d orbitals of the sulfur atoms. To further understand the roles played by heteroatoms of oxygen and sulfur in nonlinear optical materials design, molecules 1 and 2 were synthesized (Scheme I). The molecules are not directly comparable due to the relationship of the oxygen and sulfur atoms to each other. In compound 1 the oxygen atoms are meta to each other, while in compound 2 the sulfur atoms occupy a para orientation to each other. The comparison is instructive, however, since these two molecules closely resemble the repeat units of the poly(p-phenylenebenzobisoxazole) (PBO) and poly(p-phenylenebenzobisthiazole) (PBZT) polymers, respectively. The samples used for DFWM measurements were fabricated via a fast melt quenching technique. Attempts to produce optical quality films by vacuum deposition were unsuccessful due to the formation of microcrystals in the deposited material. The  $\gamma$  values,  $\chi^{(3)}$  values, and dominant UV-vis absorption peaks are listed in Table II. A meaningful comparison of these values with those obtained for PBT and PBO is not possible. A recent study of PBT<sup>3a</sup> showed that previously obtained  $\chi^{(3)}$  values were underestimated due to poor film quality. The new reported

(4) Evstaf'ev, V. P.; Braz, G. I. *Chem. Heterocycl. Compd. (USSR) (Eng. Transl.)* 1970, 6, 682.

(5) Wolfe, J. F.; Loo, B. H.; Arnold, F. E. *Macromolecules* 1981, 14, 915.

(6) Martin, K. J. *Am. Chem. Soc.* 1958, 80, 233.

(7) Osman, M. J. *Chem. U.A.R.* 1971, 14, 475.

(8) Manecke, G.; Brandt, L.; Kossmehl, G. *Makromol. Chem.* 1977, 178, 1745.

(9) Rustagi, K. C.; Ducuing, J. *J. Opt. Commun.* 1974, 10, 258.

Table II. Experimental Results for Model Compounds<sup>c</sup>

compd	$\lambda_{\max}$ , <sup>a</sup> nm	$\gamma$ , esu	$\chi^{(3)}$ , esu
1	347.6 (2) <sup>b</sup> 331.8 (1)	$7.1 \times 10^{-35}$	$7.3 \times 10^{-13}$
2	364.6 (3) 347.2 (1) 332.6 (2)	$2.1 \times 10^{-34}$	$2.0 \times 10^{-12}$
3	370.2 (3) 351.4 (1) 336.0 (2)	$1.5 \times 10^{-34}$	$1.4 \times 10^{-12}$
4	390.6 (3) 372.0 (1) 355.2 (2)	$1.1 \times 10^{-33}$	$9.5 \times 10^{-12}$
5 <sup>c</sup>	394.4 (2) 375.8 (1) 359.6 (3)	$2.5 \times 10^{-33}$ $\pm 6.3 \times 10^{-34}$	$9.3 \times 10^{-12}$ $\pm 2.2 \times 10^{-12}$
6	407.2 (3) 386.8 (1) 369.0 (2)	$1.4 \times 10^{-33}$	$1.6 \times 10^{-11}$
7	430.0 (3) 405.2 (2) 383.8 (1)	$3.4 \times 10^{-33}$	$4.0 \times 10^{-11}$
8 <sup>c</sup>	370.2 (1) 243.8 (2)	$2.1 \times 10^{-33}$ $\pm 2.3 \times 10^{-34}$	$1.4 \times 10^{-11}$ $\pm 1.0 \times 10^{-12}$
9	413.6 (2) 393.0 (1)	$2.2 \times 10^{-33}$	$2.1 \times 10^{-11}$
10 <sup>d</sup>	433.4 (2)	$4.7 \times 10^{-33}$ (sol)	$4.3 \times 10^{-11}$ , $\pm 5.5 \times 10^{-12}$ (sol)
11	409.8 (1) 450.0 (shoulder) 426.5 (1)	$2.9 \times 10^{-33}$ (film) $1.4 \times 10^{-32}$	$2.4 \times 10^{-11}$ (film) $8.9 \times 10^{-11}$

<sup>a</sup> Measured on THF solutions. <sup>b</sup> Numbers in parentheses designate relative peak intensities. <sup>c</sup>  $\gamma$  values were measured in THF solution. All other measurements were made on thin films. <sup>d</sup> Measured in both THF solution and as a vacuum-deposited film. <sup>e</sup> Experimental errors are given only for those compounds measured in solution. Experimental errors produced from film measurements are estimated to be in the range 10–25%.

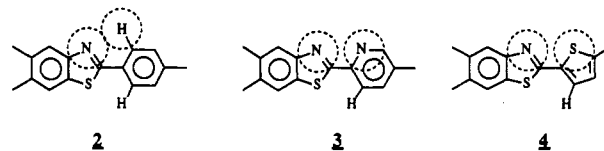
value for  $\chi^{(3)}$  of PBT was  $4 \times 10^{-10}$  esu.

The UV-vis absorption spectra for compounds 1 and 2 exhibit multiple peaks, indicating complex electronic transitions occurring in this system. In general the spectrum for compound 2 is red-shifted with respect to compound 1. This result can be explained in terms of the effect of the central benzobisthiazole or benzobisoxazole units in the molecules. A similar effect was noted in our previous work where benzothiazole, benzoxazole, and benzimidazole and their related compounds were studied.<sup>1</sup> In both the benzobisthiazole and benzobisoxazole units the heteroatoms of sulfur, nitrogen, and oxygen can donate p electrons to the molecular  $\pi$ -orbitals. However, since the electronegativity of the sulfur atom is not much different from that of the carbon atom and the electronegativity of the oxygen atom is much greater than that of the carbon atom, the distribution of the electron density will be more equally shared between sulfur and carbon in molecule 2 than between oxygen and carbon in molecule 1. Consequently, the  $\pi$ -orbitals in any sulfur-containing heteroaromatic are better delocalized than the  $\pi$ -orbitals of similar structures containing oxygen. In the case of sulfur, an important factor may also be the presence of empty d orbitals that can contribute to the molecular  $\pi$ -orbitals. The effect of this contribution will also be a reduction in the energy of the  $\pi\pi^*$  transition. As a result, it is expected that molecule 2 should have red-shifted absorption peaks when compared to molecule 1 and consequently 2 should have a larger  $\gamma$  value.

The results obtained from DFWM measurements on molecules 1 and 2, as well as the results from our previous studies,<sup>1</sup> indicate that molecules containing aromatics with sulfur atoms have higher nonlinearities than those of similar structure with oxygen atoms. Therefore, it seems advantageous to investigate the nonlinearities of those

$\pi$ -electron systems containing benzobisthiazole rather than benzobisoxazole units.

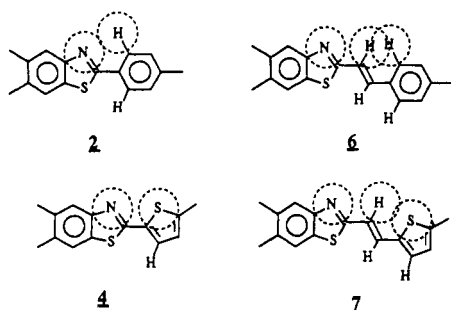
**2.2.2. Roles of Benzene, Pyridine, and Thiophene Units.** Molecules 2–4 are built with the same central unit of benzobisthiazole and the different end units of benzene, pyridine, and thiophene, respectively. As a result, the three molecules are observed to have different maximum absorption peaks and  $\gamma$  values. The red-shift of absorption peaks and the increase of  $\gamma$  values in the order of molecules 2–4 may be due to the different degree of overlap of the



$\pi$ -electron system between the central unit and the end units. Since there are hydrogen atoms attached to the carbon atoms ortho to the point of attachment of the aromatic end groups, the steric hindrance of a benzene ring is considered to be much larger than the example of an aromatic ring with only one adjacent carbon atom with a hydrogen and one heteroatom ortho to the point of attachment. This decreased steric hindrance of the heterocyclic terminated molecules leads to a more planar molecule increasing the  $\pi$ -molecular overlap and enhancing the effective conjugation in molecules 3 and 4. This increased planarity is also demonstrated by the increased red-shift of the UV-vis absorption peaks of molecules 3 and 4 in Table II. If effective conjugation were the only factor operating, it would be expected that  $\gamma$  should increase in order from compound 2 to compound 4. However, the value of  $\gamma$  for the pyridine substituted compound is slightly lower than for its phenyl-substituted counterpart. This decreased nonlinearity in 3 is possibly due to the increased electronegativity of the nitrogen atom, which causes the electrons in the pyridine ring to be somewhat more tightly bound and more difficult to polarize. The exceptionally large magnitude of  $\gamma$  for compound 4 when compared to compounds 2 and 3 is attributed to the thiophene ring and the participation of the empty 3d orbitals of sulfur. The participation of these atomic orbitals may help to lower the transition energy of the  $\pi$ -molecular orbitals. The different impact that benzene and thiophene units have on a molecule's nonlinearity is observed in other model compounds such as molecules 6 and 7. These molecules have similar structures except for the difference in the end groups. In comparison to molecules 2 and 4, the different end groups (benzene, thiophene) of 6 and 7 are the cause of the different spectral and NLO properties. The more red-shifted absorption in molecule 7 as well as a higher  $\gamma$  value may be interpreted by its effective  $\pi$ -conjugation length as discussed for molecules 2 and 4. In general, thiophene units appear to be superior to the other single ring aromatic groups studied for building new third-order NLO compounds.

**2.2.3. Role of the Ethylenic Double Bond.** Introduction of double bonds to a molecule increases its  $\pi$ -conjugation length; thus, its optical nonlinearity is enhanced. Compound 6 is constructed with two more double bonds in comparison to molecule 2. As a result, the  $\pi$ -electron transitions are red-shifted in molecule 6. Similarly, the longer  $\pi$ -conjugation length of molecule 7 results in a red-shift in the UV-vis spectra as well as a larger  $\gamma$  value in comparison to molecule 4 since the former has two more double bonds. It should be noted here that the  $\gamma$  increase from molecule 2 to molecule 6 is larger than the increase from molecule 4 to molecule 7. This difference

in the behavior may in part be attributed to measurement errors which we estimate to be 10–25% (technical note: ratio of 6 to 2 = 6.66; ratio of 7 to 4 = 3.09; worst case estimate of error of 25% will be ratio of  $0.75\gamma_6/(1.25\gamma_2) = 4.0$ , ratio of  $1.25\gamma_7/(0.75\gamma_4) = 5.15$ , which inverts the ordering of the ratios). Although the steric interactions between the fused heterocyclic ring and the hydrogen atoms in compound 2 are relieved by the addition of the double bond between the central heterocyclic unit and the terminal phenyl rings, a new steric hindrance develops between hydrogens on the double bonds and those of the phenyl ring. It seems apparent that the steric interactions (degree of planarity) between the heterocyclic ring and the double bond have greater impact on the extent of conjugation ( $\pi$ -orbital overlap) and therefore on the nonlinearity. Recent experimental single-crystal X-ray structural data<sup>10</sup> for model compounds similar in structure to 4 and 7 establish the conformation of compound 7 to be as depicted in the following: It should be mentioned here that the



conformation of compound 7 is fixed by the greater stability of the trans arrangement of the double bonds involved. The steric interactions between the fused heterocyclic ring and the next unit in compound 4 are very similar to those observed in compound 7. Therefore, there is little change in planarity by the addition of the double bond. The increase in  $\gamma$  is realized primarily because of the increase in  $\gamma$  is realized primarily because of the increase in the overall length of conjugation.

**2.2.4. Role of Pendant Alkoxy Groups.** Introducing electron-donor groups such as alkoxy to a NLO material is another way to enrich the electron densities in its  $\pi$ -conjugated backbone and thus to enhance its nonlinearity. In addition, the introduction of the pendant alkoxy groups makes the molecule more soluble in organic solvents and modifies its physical properties. As a result, third-order NLO measurements of some of these materials can be made on solutions. It is also possible to produce high-optical-quality vacuum-deposited films. One negative side effect of the incorporation of alkoxy groups is the reduction of the bandgap.

If the experimental second hyperpolarizabilities of molecules 2 and 5 are compared, it is seen that the incorporation of decyloxy groups ( $-\text{OC}_{10}\text{H}_{21}$ ) as pendant groups along the molecular backbone in 5 causes  $\gamma$  to be increased by 1 order of magnitude. It should be pointed out, however, that the  $\gamma$  value for molecule 2 was calculated from experimental data on measurements from melt quenched films. This measurement carries a relatively large error due to the less than optimal optical quality of the film and the fact that the thickness of the film is difficult to measure accurately. The measurements for molecule 5 are made on THF solutions. Although the decyloxy groups enhance solubility, the solubility is still not good enough to make measurements on widely varied solution concentrations. Consequently, a relatively large

error also exists for this determination.

Despite the possible errors in the measurements the difference in  $\gamma$  of the two compounds is still too large to be neglected. There are two opposite effects generated by the introduction of the decyloxy groups to molecule 5. The introduction of the electron donor groups ( $-\text{OC}_{10}\text{H}_{21}$ ), as already mentioned, enriches the electron density of the  $\pi$ -conjugated backbone and thus enhances its nonlinear optical behavior. In contrast, the introduction of the long-chain pendant groups might be predicted to cause increased steric hindrance between the substituted benzene rings and the central heterocyclic unit. Such steric hindrance (that is, out-of-plane rotation of the phenyl ring) would tend to decrease the optical nonlinearity due to the reduction of the  $\pi$ -electron conjugation. Experimental results show that the net interaction of the two opposite effects enhances the optical nonlinearity. The comparison of the UV-vis spectra obtained from molecules 2 and 5 indicates a more red-shifted  $\lambda_{\text{max}}$  for the latter, which implies a longer  $\pi$ -conjugation length for 5. Single-crystal X-ray structural studies of heterocyclic model compounds containing decyloxy pendant groups are currently underway to shed more light on the structural characteristics of these molecules.

Molecules 6 and 11 have similar structures except for the methoxy group substitutions on the terminal phenyl rings of 11. This substitution affects both the NLO properties and other physical properties. It is difficult to make high-optical-quality films from compound 6 because of microcrystallization. The incorporation of methoxy groups in compound 11 facilitates the processing which allows the production of films with much higher optical quality.

The methoxy groups (electron donors) in molecule 11 enrich the electron density along the molecular  $\pi$ -conjugated backbone, which in turn favors the enhancement of optical nonlinearity. This is observed in the red-shifted absorptions in the UV-vis spectra for molecule 11 in comparison to molecule 6.

**2.2.5. Benzene as a Pendant Attached to a Double Bond.** In the preceding sections the effect of lone electron pair donor groups such as alkoxy pendants in nonlinear material design has been discussed. While these groups provide lone electron pairs to the molecular  $\pi$ -conjugated backbone, which thus enhances optical nonlinearity, their presence also decreases the molecular bandgap. The narrowness of the optical transparency window is an unfavorable parameter for the nonlinear optical materials to be utilized in device design. It is for this reason that is necessary to attempt to find materials with unique structures that allow increased optical nonlinearity without lowering the bandgap.

Two different types of molecules were synthesized which were initially designed to have some "two-dimensional" conjugation. These different types are exemplified by molecules 8–10. One method of incorporating more two-dimensional character into the molecular backbone is to use pendant groups that are themselves  $\pi$ -conjugated. Molecule 8 has two pendant phenyl groups attached to the connecting double bonds between the central heterocyclic ring system and the terminal phenyl rings. The substitution of these two phenyl groups into molecule 8 does little to increase solubility or to improve film optical quality over molecule 6. Measurements on the two films indicate that compound 8 has a  $\gamma$  value that is twice that of compound 6.

Although the increase of  $\gamma$  from molecule 6 to molecule 8 is not as significant as that from molecule 6 to 11, which

(10) Fratini, A. V. Private communication.

is methoxy-substituted, a few important issues are worthy of notice. First, the UV-vis spectra indicate a blue-shifted  $\lambda_{\max}$  for compound 8 when compared to compound 6. This implies that molecule 8 has a wider transparency window than molecule 6. The blue-shifted electron transition for molecule 8 is much farther away from the laser wavelength of 602 nm used for the experimental measurements than the electronic transition of molecule 6. Second, for a one-dimensional NLO material, its second hyperpolarizability is believed to be dependent on its  $\pi$ -conjugation length.<sup>11</sup> The blue-shifted  $\pi$ -electron transition for molecule 8 implies that its  $\pi$ -conjugation length decreases and thus its  $\gamma$  should decrease. Thus, a larger value of  $\gamma$  for compound 8 is hardly expected from a one-dimensional model.

In this case, we must consider molecule 8 as a two-dimensional structure to interpret the results. In our previous investigation,<sup>1</sup> we attributed a similar behavior to the contributions to the orientationally averaged second hyperpolarizability from other tensor components of  $\gamma$  than that corresponding to the longest molecular direction ( $z$  direction). Indeed, in a two-dimensional molecule there is also a minor contribution from the  $\pi$ -conjugated branches along the  $x$  direction (if the molecule is considered to be in the  $xz$  plane). Relevant components of  $\gamma$  will be  $\gamma_{zzzz}$ ,  $\gamma_{xxxx}$ , and  $\gamma_{xxzz}$  with the averaged hyperpolarizability containing all three contributions. Hence attaching  $\pi$ -conjugated side groups may be a good way to enhance the optical nonlinearity while maintaining a wide window of transparency.

**2.2.6. Benzobisthiazole vs. *N,N*-Diphenylbenzobisimidazole.** In our previous work<sup>1</sup> we compared the influence of benzothiazole and benzimidazole units on the molecular nonlinearity when they are incorporated into various structures. When comparing the two units, whether independently or as a building block of a larger molecule, benzothiazole always appears to be a better NLO unit than benzimidazole. In contrast, when *N*-phenylbenzimidazole is used as a structural unit to build NLO materials, it appears to have a higher NLO activity than a benzothiazole unit. This unit also provides increased solubility while maintaining the width of the optical transparency window. As part of the subject study we have made a comparison of molecules containing benzobisthiazole structural units with those containing *N,N*-diphenylbenzobisimidazole units.

As discussed in section 2.2.1 molecule 2 has a larger  $\gamma$  value than molecule 1 because of the different central heterocyclic units in the respective structures. This result indicates that benzobisthiazole is a better nonlinear optical building block than benzobisoxazole. Similarly, it may be inferred that the benzobisthiazole unit should also be a better NLO block than benzobisimidazole due to the presence of empty 3d orbitals of the sulfur atom of the former unit. However, the *N,N*-diphenylbenzobisimidazole unit, as a NLO material building block, functions quite differently from benzobisimidazole. Molecules consisting of the *N,N*-diphenylbenzobisimidazole unit (e.g., molecules 9 and 10) not only have higher optical nonlinearity than similar molecules containing benzobisthiazole (e.g., molecules 6 and 7) but also have greatly improved solubility. Moreover, the pendant benzene units in molecules 9 and 10 cause almost no shift in the  $\pi$ -electron absorption spectra when compared to molecules 6 and 7 in which the sulfur atoms in the central unit usually cause 6 and 7 to

**Table III. Comparison of Theoretically Calculated and Experimentally Measured  $\gamma$  Values for Representative Model Compounds**

compd	exptl $\gamma$ , esu	theoret	
		conformation	$\gamma$ , esu
2	$2.1 \times 10^{-34}$	staggered	$2.52 \times 10^{-34}$
		planar	$1.248 \times 10^{-33}$
6	$1.4 \times 10^{-33}$	trans, staggered	$1.026 \times 10^{-33}$
		cis, staggered	$1.064 \times 10^{-33}$

absorb at a longer wavelength.

Molecules 6 and 9 have similar terminal structures but different central units. Their very similar absorption spectra indicate that they have roughly the same  $\pi$ -conjugation length. For molecule 9, however, the pendant benzene units give the molecule a two-dimensional character even though the branches are short. The  $\gamma$  value for the molecule has a contribution not only from its longest  $\pi$ -conjugated backbone direction ( $z$ ) but also from the branched conjugated direction ( $x$ ). In this case, the orientationally averaged  $\gamma$  value for molecule 9 is the combination of the  $\gamma_{zzzz}$ ,  $\gamma_{xxxx}$  and  $\gamma_{xxzz}$ . In addition, the branched benzene groups, as  $\pi$ -electron donors, will also enrich the  $\pi$ -electron density along the longest  $\pi$ -conjugated direction. This conformation favors the enhancement of the  $\gamma_{zzzz}$  value. If molecule 9 did not have the branched benzene groups, the molecule would be predicted to have a smaller  $\gamma$  value than molecule 6 since benzobisimidazole is not considered to be as good of a nonlinear building block as benzobisthiazole.

Molecule 9 also has improved properties for the preparation of thin films by vacuum deposition. Films of reasonable quality have been prepared by using compound 6, but films prepared from compound 9 are of much better quality which thus minimizes experimental error.

In a similar comparison of the structure of molecules 7 and 10, their central units cause variations in their physical, spectral, and nonlinear properties. Molecule 10 has such an increased solubility that measurements may be performed in THF solution or on high-quality optical films. Measurements on both these sample forms give basically the same experimental values for  $\gamma$  (Table II). An additional experimental observation of compound 10 is the presence of a blue fluorescence that results from a two-photon absorption. In this case, the measurements are not claimed to provide a true nonresonant  $\gamma$  value since excited states produced by two-photon absorption will contribute to the DFWM signal.

**2.3. Conclusion.** It was demonstrated that the second hyperpolarizabilities of organic molecules may be substantially improved if proper functional groups are chosen for incorporation into the building blocks for a particular molecule. The experimental values of  $\gamma$  are in some cases in good agreement with those previously calculated<sup>11</sup> by using a semiempirical method involving a MNDO approximation with the finite-field (FF) approach. Since this method utilizes a static field, the calculated  $\gamma$  values are static molecular hyperpolarizabilities that represent either the extrapolation to low frequency or a nonresonant case. Table III lists the experimentally determined and theoretically calculated  $\gamma$  values for two representative model compounds (compounds 2 and 6). The conformational structures assumed in the theoretical calculations are also specified in the table. For molecule 2, the experimental  $\gamma$  value is very close to the calculated value by assuming a staggered structure. The experimental results in Tables II and III indicate that molecule 2 adopts the more favorable staggered structure as discussed in section 2.2.2. If the staggered conformation is assumed for molecule 6,

(11) Goldfarb, I.; Medrano, J. In *Nonlinear Optical Effects in Organic Polymers*; Messier, J., Kajzar, F., Prasad, P., Ulrich, D., Eds.; Kluwer Academic Publishers: Dordrecht, 1989; p 93.



the slightly larger experimental value versus the theoretical value implies that this molecule may adopt a conformation somewhere between the planar and the staggered extremes. In general, the studies on the systematically synthesized materials lead to the following conclusions:

(i) Molecular second hyperpolarizabilities in quasi-one-dimensional molecules increase very rapidly with the  $\pi$ -conjugation length along the backbone direction. One way to achieve the goal of high  $\gamma$  is the introduction of double bonds or other  $\pi$ -electron-rich groups into the molecular backbone.

(ii) Inclusion of a sulfur heteroatom in the  $\pi$ -conjugated system may favor the enhancement of the nonlinearity because of either the participation of empty d orbitals or the release of steric interactions between each block unit. Sulfur containing aromatic links such as thiophene are more nonlinear than those aromatic links containing nitrogen and/or oxygen atoms.

(iii) *N,N*-Diphenylbenzimidazole is a better NLO block unit than benzobisthiazole. Materials made from the former structural block units convert the molecular structure from one having one-dimensional  $\pi$ -electron conjugation to one having a two-dimensional character. As a result, these materials have enhanced third-order optical nonlinearity without reducing the transparency window. The film-forming characteristics and solubilities in this class of materials are improved as well.

### 3. Experimental Section

All solvents, commercially available, were distilled and stored over molecular sieves (Linde 4A) before use. All other reagents were used without further purification. Thin layer chromatography (TLC) was performed either on precoated plastic silica gel strips with UV-254 indicator (Beckmann Instruments, Inc., Westbury, NY) or on glass-precoated KC18 reverse phase plates with UV-254 indicator (Whatman, Ltd.). Melting points were uncorrected. Electron impact mass spectra (EIMS) were performed on a Finnegan GC/MS/DS Model 4021 system. Physical properties, elemental analyses, literature references, and mass spectral data for all model compounds are summarized in Table I.

**3.1. Procedure A.** A solution of tri-*n*-butylamine (21.78 g, 0.118 mol) was added dropwise to a mixture of 2,5-diamino-1,4-benzenedithiol (7.21 g, 0.029 mol), the appropriate carboxylic acid (0.059 mol), PPSE (24.0 g), and *o*-dichlorobenzene (60 mL) under nitrogen atmosphere. Upon completion of the addition of amine the temperature of the reaction was increased to 85 °C and maintained there for 24 h. At the end of this period the reaction temperature was increased to 135 °C for an additional 24 h. The reaction mixture was cooled to room temperature and poured into methanol (700 mL). The resulting precipitate was filtered, washed with additional methanol (300 mL), and allowed to air dry for several hours. The crude product was further purified by recrystallization from the appropriate solvent (Table I).

**3.2. Procedure B.** *trans*-1,7-Diphenyl-2,6-bis[2-(2-thienyl)vinyl]benzo[1,2-*d*:4,5-*d'*]bisimidazole. A mixture of 2,6-dimethyl-1,7-benzo[1,2-*d*:4,5-*d'*]bisimidazole<sup>8</sup> (6.72 g, 20.0 mmol), 2-thiophenecarboxaldehyde (60 mL), and boric acid (2.5 g) was heated at reflux under nitrogen for 12 h. The reaction mixture was poured into 95% ethanol and filtered. Washing with water and ethanol gave 6.64 g (53%) of crude product. Several recrystallizations from toluene afforded needles of high purity, mp 301–302 °C (DSC,  $\Delta T = 10$  °C/min). The purified product gave satisfactory elemental analyses and mass spectral results (Table I).

**3.3. Sample Preparation.** The  $\chi^{(3)}$  values for NLO materials were measured either in the solution or in the solid state. For many organic compounds with relatively large molecular weights the solubility in common organic solvents is greatly reduced. It is therefore impossible to accurately measure their  $\chi^{(3)}$  values from solution. Two methods are generally used to overcome such disadvantages for these materials. The first method involves the incorporation of various pendant groups to increase the free

volume of the molecule thereby increasing its solubility, and the second method is the modification of the molecular structure to enable the fabrication of high-optical-quality thin films. Therefore, in addition to our goals of understanding the relationship between structure and nonlinear optical properties and searching for those organic materials with high  $\chi^{(3)}$  values, we were also interested in the relationship between structure and mechanical properties in order to fabricate good-optical-quality films.

For the insoluble organic molecules studied in this paper, the measurements of  $\chi^{(3)}$  values were performed on thin films. Methods of vacuum deposition and melt quenching were utilized to prepare these films. The vacuum deposition was performed at a speed of between 30 and 50 Å/s in a vacuum chamber whose vacuum is kept at  $10^{-6}$ – $10^{-5}$  Torr. Very clean glass slides were used as substrates. The deposition velocity and the film thickness were monitored and estimated by using a quartz crystal film thickness monitor (Model FTM4). The thickness was also calibrated by using a profilometer (Model  $\alpha$ -4). During the deposition process, chemical decomposition for these materials was not observed since the UV-visible absorption spectra obtained from their THF solution before and after the deposition were identical. The thickness of films obtained this way were in the range 1–3  $\mu$ m.

Most materials with a relatively high molecular weight gave acceptable quality films from vacuum evaporation. Few materials, as previously discussed, gave good-optical-quality films. An important factor to determine whether the material is capable of fabrication into optical-quality film is the molecular size. It was demonstrated that molecules with certain pendant groups such as phenyl or decyloxy were more likely to produce good-quality films (see molecules 9–11). For lower molecular weight substances, the films obtained from vacuum evaporation exhibited milky or microcrystalline structures, which prohibited any DFWM measurements because of light scattering. In this case thin films were prepared by fast quenching of the compounds in the melt phase under nitrogen on microscope slides. This procedure often afforded film with reasonably good quality areas a few square millimeters in size which were used for measurements. The thickness of films obtained in this manner ranged between 10 and 30  $\mu$ m. The nonuniformity of the film, the unknown orientation of the crystalline areas, and the relatively large error in the determination of the film thickness will introduce a larger uncertainty in measurement of the  $\gamma$  values of this type of sample.

**3.4. Bandgap.** A good nonlinear optical material must possess both high optical nonlinearity and wide optical transparency window for practical applications. Both the optical transparency window and the nonresonant  $\gamma$  value for a nonlinear material are qualitatively related to each other since they both are dependent on the  $\pi$ -conjugation length. In the subject research, it was intended not only to optimize the nonlinearity through manipulation of the molecular structure but also to widen the optical transparency window of the materials. The measurement of the bandgap absorption was performed on a UV-260 spectrometer.

**3.5. Measurement of Second Hyperpolarizabilities.** The third-order optical nonlinearities can be measured by a variety of techniques. The method of choice for this investigation is that of time-resolved backward or forward geometry DFWM of either solutions or films. The system used for the measurements was identical to that described in our previous publication.<sup>3</sup> It delivers amplified nearly transform limited 400-fs limited pulses at 602 nm with a repetition frequency of 30 Hz and maximum energy of approximately 0.4 mJ/pulse. An appropriate set of beam splitters and mirrors was used to obtain three beams that were synchronized by using delay lines to be simultaneously incident at the sample. The peak power at the sample was usually in a range 1–20 GW/cm<sup>2</sup>. By delaying one of the beams (the backward beam in the backward geometry or the out-of-plane beam in the forward geometry) with respect to the other two beams, the temporal profile of the DFWM signal was recorded. The signal was observed as the phase conjugate of the probe beam in the backward geometry and in the position given by the appropriate phase-matching condition in the forward geometry case. The signal was monitored with a photodiode and processed with a boxcar averager (EG&G Princeton Applied Research, Model 4200). The data were further processed by a computer.

In all cases but one (compound 10) the signals corresponded to instantaneous (within temporal resolution) formation and decay

of the transient gratings giving rise to the DFWM signal. This is usually taken as the indication of no contribution of a population grating, which can be formed by excited states generated by one or two photon absorption. However, such a population grating was observed for compound 10.

The intensity of the DFWM signal for a solution or a film was compared to that obtained for a reference sample under identical conditions. The third-order susceptibility,  $\chi^{(3)}$ , for the solution or the film is calculated by the following equation:

$$\chi^{(3)} = \left(\frac{n}{n_r}\right)^2 \left(\frac{I}{I_r}\right)^{1/2} \frac{l_r}{l} \chi_r^{(3)} F \quad (3)$$

where  $I$  stands for the DFWM intensity,  $n$  is the refractive index of the medium,  $l$  is the interaction length, and the subscript  $r$  refers to a reference sample.  $F$  is the correction factor needed to account for absorption losses. In our measurements we found one-photon absorption at 602 nm negligible for all the investigated compounds (that is, absorbance of the films was lower than a few hundredths of a unit). Solution measurements of 10 in THF at higher concentrations showed that at such concentrations an absorption correction was necessary. This was the result of a relatively strong two-photon absorption and not one-photon absorption. This problem has been treated in a previous paper,<sup>12</sup> and we used the same correction factor as was derived there.

The reference was a 1-mm-thick cell filled with THF for which we used the value for  $\chi^{(3)}$  of  $3.3 \times 10^{-14}$  esu. This value has been adopted in our laboratory after numerous comparisons of different standards for  $\chi^{(3)}$  measurements. THF is a much more reliable standard than the commonly used CS<sub>2</sub> since the nonlinearity of THF does not depend as critically on the pulse length as in the case with CS<sub>2</sub>.

In eq 3 one assumes that the input power dependence of the DFWM signal is identical for the investigated substance and the reference. Theoretically these dependences should be cubic. The power level of the input beams was always kept at the minimum level to avoid saturation effects, contributions from fifth-order nonlinearity, and to minimize two-photon absorption.<sup>12</sup>

For film measurements, the second hyperpolarizability for a molecule can be calculated by using the following expression:

$$\chi^{(3)} = L^4 N \gamma \quad (4)$$

where  $\chi^{(3)}$  is calculated from eq 3,  $N$  represents the molecular density (i.e., the number of molecules per cubic centimeter), and  $L$  was the local field factor in the solid state.  $L$  is approximated by the Lorentz expression<sup>13</sup>

$$L = (n^2 + 2)/3 \quad (5)$$

where  $n$  is the refractive index for the material at 602 nm. The calculation of molecular density  $N$  is based on the material density, which is measured by the flotation method. The refractive indexes for the few materials that were made into good-optical-quality films, were measured by using the  $m$ -line technique.<sup>14</sup> The refractive indexes for other materials were estimated based on

the additivity of the molecular polarizability. These indexes were in the range 1.50–1.65. The error introduced by such an estimation was calculated to be less than experimental error.

For a solution measurement, the  $\chi^{(3)}$  calculated from eq 1 has contributions from the solute and from the solvent. Therefore, the third-order susceptibility for the solution was treated as the sum of the two contributions:

$$\chi^{(3)} = L^4 (N_s \gamma_s + N_x \gamma_x) \quad (6)$$

where  $\gamma_s$  and  $\gamma_x$  stand for the second hyperpolarizabilities of the solvent and solute, respectively,  $N_s$  and  $N_x$  denote the respective molecular densities, and  $L$  is the local field factor in the solution state, which is approximated by using the Lorentz expression. The refractive index  $n$  in the Lorentz expression was measured by using an Abbe refractometer at the sodium line (589 nm). No dispersion correction was attempted.

For soluble compounds, the  $\chi^{(3)}$  values at different concentrations were calculated by using eq 3 and the  $\gamma$  values were obtained by a least-squares fit to eq 6. Errors of the determination of  $\gamma$  were calculated by consideration of the uncertainties of the measurements of the DFWM intensities for individual points. Other experimental factors such as the concentration range, the concentration intervals, the number of solutions, and the laser instability may also induce different errors under different conditions.

Equation 6 is assumed to hold true for the case when the solution nonlinearity is composed of coherent contributions of real parts of the hyperpolarizabilities of the solute and the solvent. This assumption breaks down in the presence of either one- or two-photon absorption and there appear contributions from both the real and the imaginary parts of the hyperpolarizability of the solute.<sup>15</sup> In this case, the derived  $\gamma$  values were treated as effective quantities, and the following equation for fitting the concentration dependence was used:<sup>15</sup>

$$|\chi_{eff}^{(3)}| = L^4 ((N_1 \gamma_{1r} + N_2 \gamma_2)^2 + (N_1 \gamma_{1i})^2)^{1/2} \quad (7)$$

where  $\gamma_{1r}$  and  $\gamma_{1i}$  represent the real and the imaginary parts for the complex second hyperpolarizability of the solute respectively and  $\gamma_2$  is the second hyperpolarizability for THF for which no imaginary part was assumed. In the present study, the best least-squares fit for the solution data for compound 8 was obtained by assuming only positive real  $\gamma$  for the solute.

**Acknowledgment.** The work performed at SUNY, Buffalo, was supported by the Air Force Office of Scientific Research, Directorate of Chemical and Atmospheric Sciences and the Polymer Branch, Materials Directorate, Wright Laboratory, through Contract Number F49620-90-C-0021. We acknowledge the assistance of Ann Dillard, University of Dayton Research Institute, for the scale-up synthesis of model compounds and the personnel of the Materials Integrity Branch, Systems Support Division, WL/MLSA, for the performance and interpretation of the elemental analyses and mass spectral data.

(12) Zhao, M.; Cui, Y.; Samoc, M.; Prasad, P.; Unroe, M.; Reinhardt, B. *J. Chem. Phys.* In press.

(13) Prasad, P.; Williams, D. J. *Introduction to Nonlinear Optical Effects in Molecules and Polymers*; John Wiley & Sons: New York, 1991.

(14) Ding, T.; Garmire, E. *Appl. Opt.* 1983, 22, 3177.

(15) Shand, M. L.; Chance, R. R. In *Nonlinear Optical Properties of Organic and Polymeric Materials*; Williams, D. J., Ed.; ACS Symp. Ser. No. 233; American Chemical Society: Washington, DC, 1983.